Received: 22 June 2021 | Revised: 30 September 2021 | Accepted: 30 September 2021

DOI: 10.1002/pat.5537

RESEARCH ARTICLE

polymers for advanced technologies WILEY

Self-healing behavior in blends of PDMS-based polyurethane ionomers

Federico Da Via[1] | Raffaella Suriano[1] | Oussama Boumezgane[1] | Antonio M. Grande[2] | Claudio Tonelli[3] | Stefano Turri[1]

[1]Department of Chemistry, Materials and Chemical Engineering "Giulio Natta", Politecnico di Milano, Milan, Italy

[2]Department of Aerospace Science and Technology, Politecnico di Milano, Milan, Italy

[3]Solvay Specialty Polymers S.p.A., Bollate, Italy

Correspondence
Stefano Turri, Department of Chemistry, Materials and Chemical Engineering "Giulio Natta", Politecnico di Milano, Piazza Leonardo da Vinci 32, 20133, Milan, Italy.
Email: stefano.turri@polimi.it

Abstract

Ionic interactions offer the highest non-covalent cohesive strength in supramolecular assemblies. In spite of that, they have been consistently underestimated in the development of self-healing materials due to their lack of directionality and association specificity. In this paper, ionic moieties are introduced as side-chain pendants in poly(urea-urethane) siloxane-based polymers, aiming to obtain a strong yet flexible elastomer with the capability to recover from a damaged state. The synthesis was carried out by a two-step polymerization involving polydimethylsiloxane (PDMS) diamine-terminated, isophorone diisocyanate (IPDI) and a chain extender providing the required ionic functionality. Internal phase separation allowed the material to show its elastomeric behavior. After preparation of the blend by mechanical mixing, the formation of ionic interactions was checked for by FT-IR spectroscopy, rheological analysis and tensile tests. Healing of notch damage was evaluated both with respect to tensile strength and fracture toughness. At room temperature (21°C) and humidity (30% RH) the maximum recovery measured at 14 days was 47%. Self-healing dependence on humidity and temperature was assessed, resulting in further improvements (up to 100%) as molecular mobility was increased by both conditions.

KEYWORDS
ionomers, mechanical properties, polydimethylsiloxanes, polyurethanes, self-healing

1 | INTRODUCTION

In past years, supramolecular chemistry has gained popularity in material science, as noncovalent interactions allow to add peculiar behaviors to otherwise covalent systems. Its main attractiveness is the low energy barrier existing between the associated and dissociated state of molecules, resulting in accessible reversibility.

In polymer chemistry, noncovalent interactions have been successfully used both as main-chain[1] and side-chain[2] connections for supramolecular polymer networks (SPN). Further classification is determined by the physical nature of the reversible interactions: π–π stacking,[1] hydrogen bond,[2] metal–ligand coordination[3] and ionic interaction[4,5] are the categories currently reported.

Polymers containing ionic moieties as chain pendants, with concentration below 15% w/w, are termed ionomers. Whilst they found extensive application as coatings for their improved Young's modulus and toughness,[6] the literature on the development of ionomeric self-healing materials is still quite slim. As presented in the Eisenberg–Hird–Moore model,[7] ionic interactions between polymeric chains are formed by aggregation of oppositely charged moieties into clusters by

electrostatic attraction. This association mechanism is controlled only by cluster size, with no mutual recognition of interacting couples. Despite the high cohesive strength, the lack of directionality and association specificity is viewed as detrimental to a more diffused adoption. Ionomers can bear a single charge type, identifying cationomers and anionomers, or both of them, in so-called zwitterionomers.

In this framework, polyurethanes assumed great relevance in the field of ionomers, exploiting their intrinsic superior mechanical properties. Moreover, nitrogen, oxygen and hydrogen atoms in the urethane group can increase the overall supramolecular cohesion by charge-assisted hydrogen bonding.

Tertiary amines can provide cationic functionalities by activation through quaternization reaction from an initial neutral charge. The most-reported methodology involves chain-extension of the polyurethanes prepolymer by N-methyldiethanol amine (MDEA)[8] with quaternization by a strong acid, such as HCl[9] or acetic acid.[10]

For polyurethane anionomers, early practice contemplated the use of chain-extenders with acid side-chain functionalities of high dissociation constant, as sulphuric[11] or phosphoric[12] acid. Chain-extender selection also included carboxylic acid functionalities,[13,14] aiming to dampen the unfavorable effect of acid proton dissociation on the urethane polymerization kinetics. Alternative routes of synthesis revolved around post-functionalization of otherwise non-ionic polyurethanes.[15–17]

Zwitterionomeric polyurethanes synthetic path for the most part relies on the work of Cooper et al.[18–22] Cationic centers are provided by means of MDEA chain-extender, subsequently ionized by 1,3-propanesultone bonding to tertiary amine sites.

Self-healing behavior in ionomeric polyurethanes is based on the spontaneous re-assembly of ionic clusters, both positive and negative centers being required. Zwitterionomers proved to be ready-made for the purpose as a single macromolecule carries both ionic species, reducing the number of steps and variables in material synthesis. The experimental layout has been set by Chen et al.[23,24] with the aforementioned functionalization with 1,3-propanesultone. Alternative methods described the formulation of polyurethane supramolecular assemblies comprised of a macromolecular polyurethane ionomer, cationic or anionic, with a micro-molecular counterion.[25]

Attempts to blend different ionomers to achieve ionic crosslinking and interpenetrated polymer network (IPN) microstructure were limited and focused on Lewis acid–base pairs[26,27] or without evaluation of possible self-healing phenomena.[28] Very recently, a 3D printable PDMS-based hybrid system[29] has been proposed, mixing covalently and ionically crosslinked species.

Considering this background, a novel poly(urea-urethane) based on a PDMS main-chain was developed, showing elastomeric behavior at room temperature. Tertiary amines or carboxylic acid pendants were used for ionic functionalization. The blending procedure of the two ionic components, by hot mechanical mixing, proved to be efficient, solvent-free and in line with future industrial production. Differently from previously examined systems,[23–25,30,31] the flexibility from the PDMS backbone contributed to achieve a significant self-healing behavior, as diffusion limitations could have hindered the spontaneous reassembly of ionic clusters in a completely macromolecular system.

2 | EXPERIMENTAL

2.1 | Materials

(3-Aminopropyl)-terminated polydimethylsiloxane(PDMS-NH_2) (DMS-A15, MW = 3000 g/mol) was purchased from Gelest Inc. (USA) and dried by heating under vacuum for 4 h at 90°C. All other chemicals were purchased from Sigma-Aldrich (Germany) and used as received, except for solvent tetrahydrofuran (THF) and dimethylformamide (DMF), dried by means of 4 Å molecular sieves for at least 24 h under nitrogen atmosphere.

2.2 | Synthesis of PDMS-based poly(urea-urethane) ionomers

PDMS-based poly(urea-urethane) synthesis was carried out in a two-step process, divided into pre-polymerization and chain-extension, both schematized in Figure 1.

Equipment was comprised of a round bottom flask, equipped with an Allihn condenser and glass stirring shaft. The system was kept under dry atmosphere by means of a nitrogen flux.

Prepolymerization was carried out in the same fashion for both cationomer and anionomer. First, isophorone diisocyanate (IPDI) was dissolved in THF, the solvent corresponding to 30% w/w to the final expected dry polymer. PDMS-diamine was added by dripping under stirring, using a pressure-equalizing dropping funnel. The molar ratio was defined with an excess of IPDI ($NCO/NH_2 = 1.5$). Reaction conversion was monitored by Fourier transform infrared (FT-IR) spectroscopy to an isocyanate content plateau.

For the cationomer, chain extension was carried out by the addition of 3-(dimethylamino)-1,2-propanediol in slight excess with respect to theoretical NCO residual content ($OH/NCO_{RES} = 1.1$). Catalyst was added, with load of dibutyltin dilaurate (DBTDL) corresponding to 0.1% w/w of IPDI and the reaction proceeded at 45°C up to the complete disappearance of NCO absorption (approximately 22 h). For the anionomer, the chain extender used was 2,2-bis(hydroxymethyl) propionic acid (DMPA) dissolved in DMF. The catalyst load corresponded to 0.6% w/w of IPDI. The reaction was carried out at 60°C up to complete NCO conversion (approximately 42 h).The solvent was removed from the final polymer by drying under vacuum at 60°C.

IR (NaCl): υ (cm^{-1}) = 3340 (N—H), 2962 (C—H), 2258 (N═C═O), 1628 and 1572 (C═O), 1090 and 1022 (Si—O).

2.3 | Blend preparation

Blending of cationomer and anionomer took place by hot mechanical mixing in a Brabender Plasti-Corder Lab Station equipped with type 350e mixer, mixing parameters being 80°C and 60 min^{-1} rotational

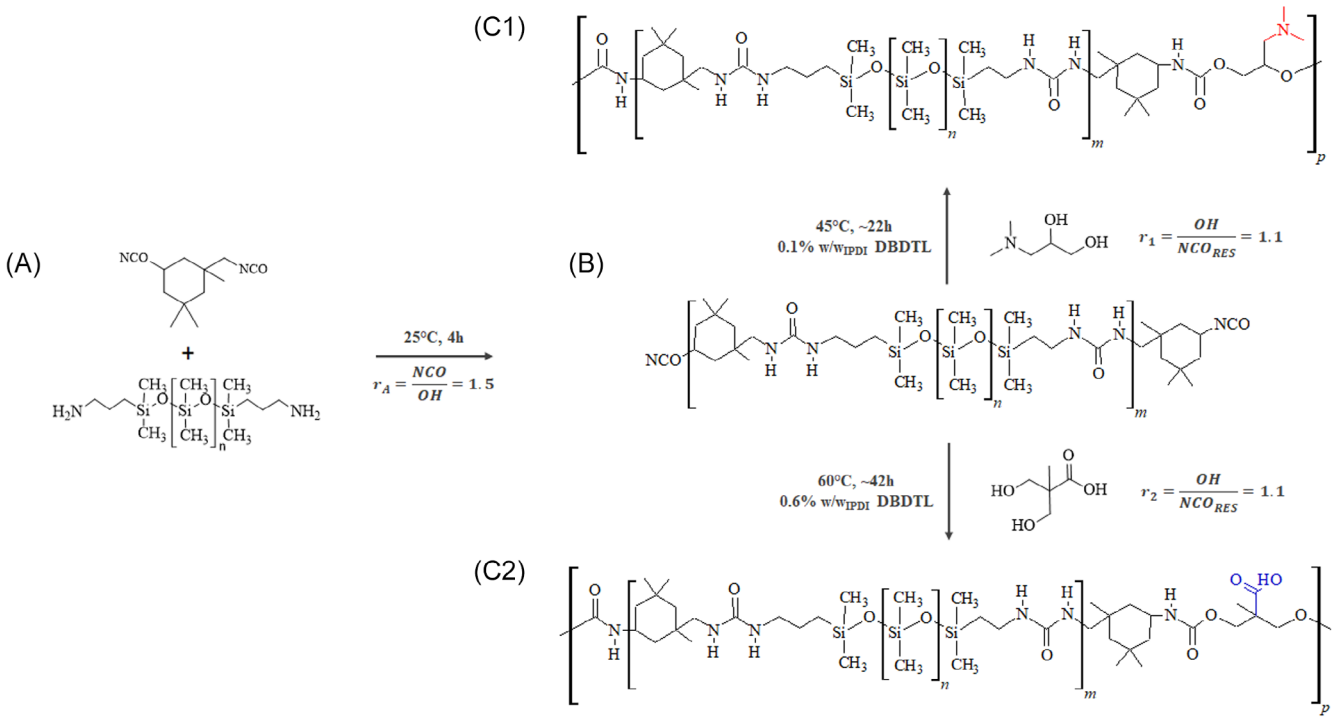

FIGURE 1 Raw ionomers synthetic path. The monomers IPDI and PDMS-NH2 (A) are combined to form the prepolymer (B). Then, they are chain-extended to give either the cationomer (C1), with tertiary amine functionality (red), or the anionomer (C2), with carboxylic acid functionality (blue). Stoichiometric coefficient rA of pre-polymerization and r1, r2 of chain extension are reported

speed. The stoichiometric ratio between equivalents of cationic and anionic functionalities was considered. Mixing proceeded to a torque plateau, indicating the achievement of homogeneous material.

Hot molding (100°C, 75 kg/cm^2) allowed to obtain flat sheets of material, with a surface area of 10 × 10 cm^2 and 2 mm thick.

Cationomeric and anionomeric poly(urea-urethane) samples were named PUU CAT1.5 and PUU ANC1.5, respectively. The resulting ionic blend was named PUU CAT1.5-ANC1.5.

2.4 | Characterization techniques

2.4.1 | FT-IR spectroscopy

Fourier-transform infrared spectroscopy was performed with a Thermofisher Scientific NICOLET 760-FTIR Nexus. Samples were prepared by film deposition onto NaCl windows, with spectra collected from 625 to 4000 cm^{-1} with 64 scans at 4 cm^{-1} resolution.

2.4.2 | Gel permeation chromatography (GPC)

The molecular weight of the final ionomer was evaluated by gel permeation chromatography, performed on an apparatus consisting of a Waters 515 HPLC pump (mobile phase THF; flow rate 1 ml/min at 35°C), three Styragel columns (model HR 4, HR 3, and HR 2) from Waters, and a refractive index detector Waters 2410. Samples were dissolved in THF at 0.2% w/w concentration. Calibration used monodispersed styrene fractions.

2.4.3 | Thermogravimetric analysis (TGA)

Thermal stability was checked for by thermogravimetric analysis on a TA Instruments Q500 from room temperature to 800°C at a heating rate of 10°C/min under nitrogen atmosphere.

2.4.4 | Dynamic mechanical analysis (DMA)

Thermal transitions were determined by dynamic mechanical analysis in shear mode and temperature sweep configuration using a Mettler Toledo DMA/STDA 861e on flat disk samples of 6 mm diameter and 2 mm thickness. Temperature sweep was performed in the −50 to 140°C range with 3°C/min as heating rate, deformation amplitude set at 5 μm and deformation frequency at 1 Hz. The maximum values of peaks for the dissipative component (G'') of the shear modulus were used to determine the glass transition temperature (T_g) values of the samples.

2.4.5 | Rheology

Viscoelastic behavior was evaluated using a TA Instruments Discovery HR-2 rheometer, equipped with 20 mm diameter parallel plate

geometry. To highlight the effect of ionic interactions on viscoelastic properties, analysis was performed at 25°C and 75°C. The linear viscoelastic range was individuated by strain ramp from 0.01% to 5% deformation at 1 Hz frequency. Material relaxation was described by frequency sweep analysis in the range from 0.1 Hz to 10 Hz at 0.1% fixed deformation.

2.4.6 | Tensile testing

Tensile tests were carried out using a Zwick/Röell Z010 dynamometer equipped with screw grips type 8354 with a maximum loading force of 10 kN. Single edge notched tear (SENT) tests used an Instron Model 4300 with a loading cell of 1 kN. The specimen indentation was around 2 mm, measured both in virgin and healed conditions.

For both tests, rectangular flat specimens of 70 mm length, 6 mm width and 2 mm thickness were used, without preload applied and elongation speed of 10 mm/min.

2.4.7 | Surface microscopy

Surface characterization used scanning electron microscopy (SEM) to inspect the notch in SENT tests, recording its size and shape. The equipment used comprised of a Hitachi TM3000 scanning electron microscope.

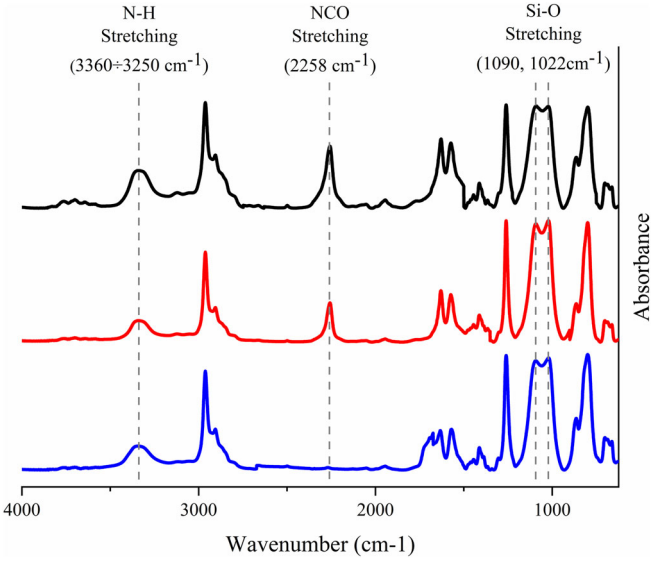

FIGURE 2 FT-IR spectra of poly(urea-urethane) ionomer synthesis: unreacted monomer mixture (top), prepolymer (middle), and chain extended polymer (bottom)

3 | RESULT AND DISCUSSION

3.1 | Synthesis monitoring

FT-IR monitoring of polymerization reaction showed behavior consistent with the formation of urethane linkages (Figure 2), with a decrease in isocyanate content (NCO stretching, 2258 cm^{-1}) to a plateau during pre-polymerization and to zero during chain extension. Molecular weights achieved resulted to be quite similar between cationomer and anionomer, with values reported in Table 1 together with composition molar ratios. A slightly lower molecular weight in the anionomeric polymer is a result of partial polymerization hindering by the presence ofcarboxylic acid functionalities[32] in the chain extender.

The material appeared completely homogeneous, colorless and transparent. Phase segregation between hard urethane and soft PDMS chains washowever present, considering the significant difference between solubility parameters[33] of PDMS (15.5 $J^{1/2}$ $cm^{-3/2}$) and urethane (37.2 $J^{1/2}$ $cm^{-3/2}$) and urea groups (45.6 $J^{1/2}$ $cm^{-3/2}$). Nevertheless, no optical scattering phenomena could be recognized, as the hard phase content was limited to 11.8% w/w for PUU CAT1.5 and 11.9% w/w for PUU ANC1.5. The hard phase content ω_{HP} was calculated as a function of IPDI, PDMS and chain extender content, here below represented as m_{IPDI}, $m_{PDMS\text{-}NH2}$, and m_{CE}, respectively:

$$\omega_{HP} = \frac{m_{IPDI} + m_{CE}}{m_{IPDI} + m_{CE} + m_{PDMS-NH2}} \quad (1)$$

Blend preparation by mechanical mixing required approximately 5 min to achieve system homogeneity, corresponding to the mixing torque plateau. The final material maintained the original colorless appearance.

In Figure 3A FT-IR spectra of the ionic blend and the pure cationomer are reported. The formation of ionic supramolecular aggregates can be evaluated by FT-IR spectroscopy, identifying an absorbance increase in two peaks situated at 1625 cm^{-1} and 1570 cm^{-1}. These two peaks can be attributed to the formation of carboxylate ions,[34] which have a greater polarity than the non-dissociated carboxylic acid pendants they are originated from. Figure 3B shows the detail of the 1750–1450 cm^{-1} range, in terms of absorbance difference percentage between the blend and the cationomer.

3.2 | Thermal characterization

In Table 2, thermal transitions are reported for ionomers and blend. All of them corresponded to the glass transition of the hard

TABLE 1 Poly(urea-urethane) ionomers molar composition and corresponding number-average (M_n), weight-average (M_w) molecular weights, and polydispersity index (PDI)

Sample	NCO/NH_2	OH/NCO_{RES}	M_n	M_w	PDI
PUU CAT1.5	1.5	1.1	26,689	42,997	1.61
PUU ANC1.5	1.5	1.1	21,176	39,067	1.85

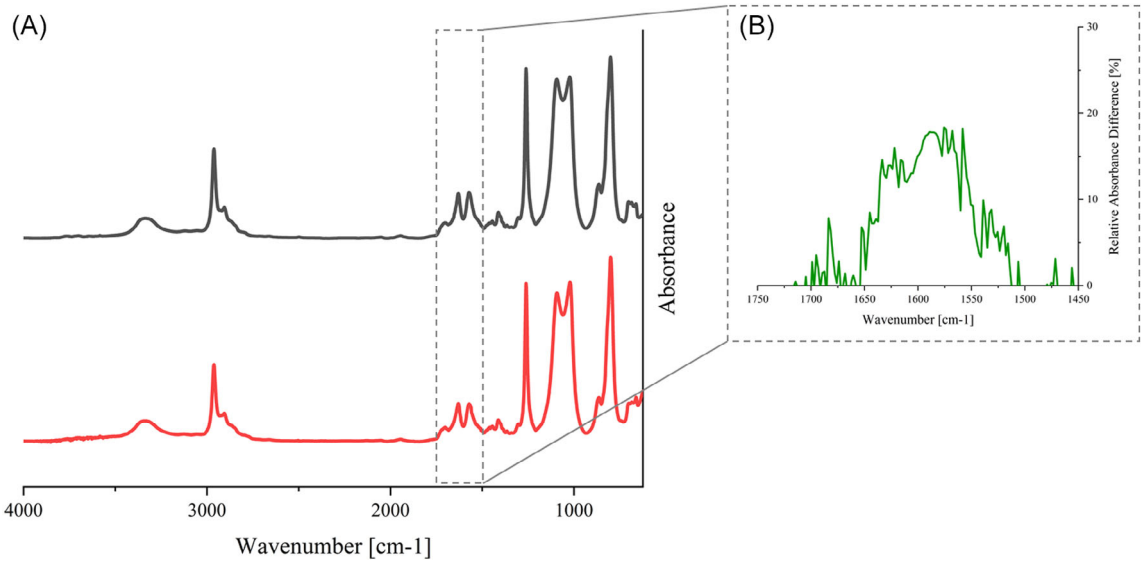

FIGURE 3 FT-IR absorption spectra (A) of PUU CAT1.5-ANC1.5 (black) and PUU CAT1.5 (red). Relative absorption difference between the two materials in the 1750–1450 cm^{-1} range (B)

Sample	T_g (°C)	T_{ONSET} (°C)	$T_{5\%}$ (°C)	Residue (800°C) (%)
PUU CAT1.5	22.9	243	281	1.0
PUU ANC1.5	31.1	267	286	0.97
PUU CAT1.5-ANC1.5	34.3	261	286	0.98

TABLE 2 Glass transition temperatures (T_g) and TGA results for poly(urea-urethane) ionomers and blend, representing degradation onset (T_{ONSET}), 5% weight loss temperature ($T_{5\%}$), and final residue weight percentage (Residue [800°C])

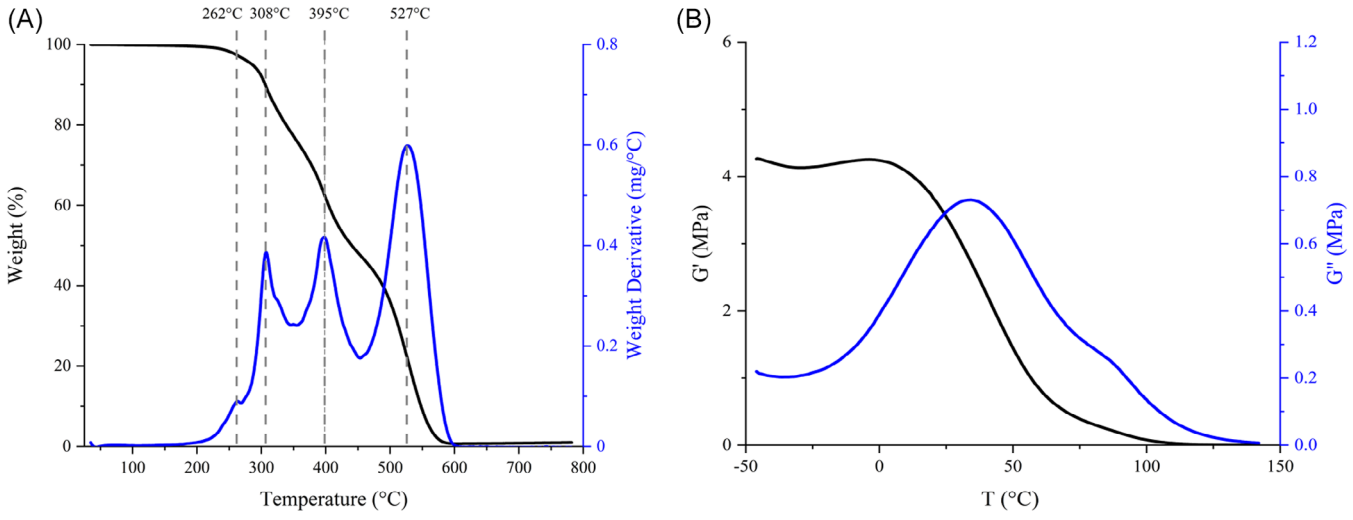

FIGURE 4 Plots for PUU CAT1.5-ANC1.5 in TGA (A) and DMA oscillatory temperature ramp (B)

TABLE 3 Shear modulus elastic (G') and viscous (G'') components at 25°C and 75°C at 0.1% deformation (linear viscoelastic range)

Sample	$G'_{25°C}$ (MPa)	$G''_{25°C}$ (MPa)	$G'_{75°C}$ (MPa)	$G''_{75°C}$ (MPa)
PUU CAT1.5	1.36	0.48	0.08	0.07
PUU ANC1.5	1.57	0.39	0.13	0.12
PUU CAT1.5-ANC1.5	1.41	0.30	0.29	0.20

phase, as the IPDI cycloaliphatic structure hinders crystalline conformational organization. Higher T_g reported for PUU CAT1.5--ANC1.5, here in Figure 4B, can be attributed to higher supramolecular cohesion inside the hard domains by the presence of ionic interactions.

The thermal stability of proposed materials was investigated by TGA, with characteristic degradation temperatures mentioned in Table 2. Polysiloxane backbone showed great thermal resistance, as the dissociation of the Si—O bond was not observed until 500°C, as shown by the TGA plot in Figure 4A. On the other side, degradation onset involved urethane linkages at around 240–260°C, defining the maximum operating temperature.

3.3 | Rheological characterization

Viscoelastic properties were evaluated to detect modifications demonstrating the presence and the effect of ionic interactions. Strain sweep was performed at both room temperature and 75°C, with data reported in Table 3. At 25°C the blend PUU CAT1.5-ANC1.5 shows an elastic shear modulus G' of 1.41 MPa, intermediate between the value measured for raw anionomer (1.57 MPa) and cationomer (1.36 MPa). On the other side, its shear modulus at 75°C resulted to be higher than both ionomers taken singularly, evidencing the reinforcing effect of ionic interactions in supramolecular cohesion. At room temperature, the presence of rigid domains hinders molecular mobility, making less relevant long-range intermolecular interactions.

Similar conclusions can be drawn from relaxation time comparison, calculated as reciprocal of crossover frequency in frequency sweep rheological tests. At 75°C, PUU CAT1.5-ANC1.5 presents a single relaxation time at 6.31 s, against 2.00 s and 0.32 s for PUU ANC1.5 and PUU CAT1.5, respectively.

3.4 | Tensile tests

Tensile tests were performed to assess the mechanical properties of the poly(urea-urethane) blend. Temperature and humidity during the testing operations were accurately controlled as the materials' glass transition was reported near room temperature, leading to undesired energy dissipation phenomena. The testing temperature was set at 21°C with 30% RH. Mechanical properties evaluated by means of tensile tests were Young's modulus (E), strain at break (ε_{Break}), tensile strength (σ_{Break}), and fracture energy (w), calculated as the area underneath of the stress–strain curve.

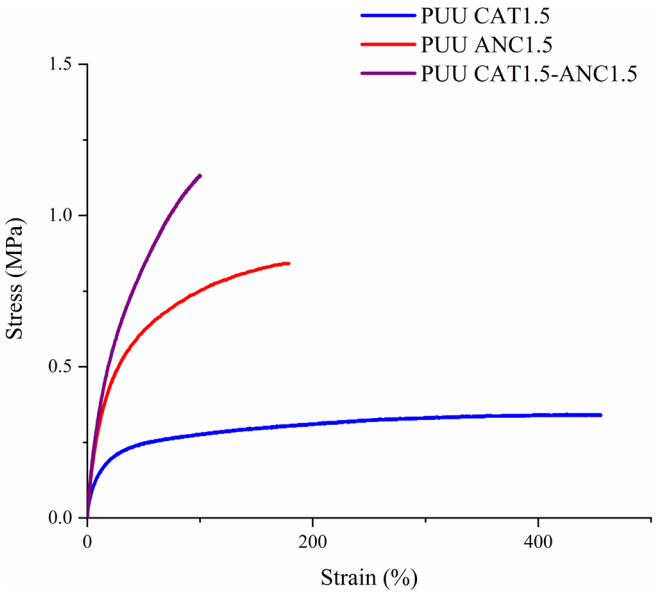

FIGURE 5 Stress–strain curves for raw ionomers and PUU CAT1.5-ANC1.5 blend

Even for temperatures well below the glass transition, a clear effect due to ionic interactions was detected, with the blend appearing more rigid as shown in Figure 5. This condition reflected in fracture properties, with higher stress and lower strain at break. In Table 4, complete mechanical properties are summarized.

The Young modulus values are in agreement with the results from rheological tests as they are intermediate between raw anionomer and cationomer values.

3.5 | SENT tests

In "soft polymers" as the material proposed in this work, structural recovery takes place mainly by interfacial diffusion across cracks. As fracture mechanics quantitatively evaluates interfacial phenomena, it should provide a better picture of the self-healing process.[35] Among existing methodologies, the elastomeric nature of the proposed ionomeric blend made single edge notch tear (SENT) tests[36–39] an acceptable and reliable choice.

Sample	E (MPa)	ε_{Break} (MPa)	σ_{Break} (MPa)	w (J/cm^3)
PUU CAT1.5	1.69	450.7	0.34	1.37
PUU ANC1.5	3.92	169.9	0.85	1.13
PUU CAT1.5-ANC1.5	3.43	100.9	1.11	0.77

TABLE 4 Young modulus (E), strain at break (ε_{Break}), tensile strength (σ_{Break}), and fracture energy (w) of poly(urea-urethane) raw ionomers and blend (21°C, 30% RH)

In this work, the following different sets of healing conditions were considered, for a better understanding of the role played by environmental parameters in healing mechanisms: room temperature/low humidity (21°C, 30% RH); room temperature/high humidity (21°C, 86% RH); oven exposure at moderately high temperature (50°C). Each sample was indented with a stainless-steel blade and the notch width was measured by SEM. Upon fracture, the two separated ends were reconnected and kept in place between two glass slides. After the set time elapsed, the notch width was measured again to consider the material residual deformation. A second tensile cycle provided the mechanical properties of the healed specimen.

In accordance with widespread practice for elastomer self-healing evaluation, two parameters were used: tensile strength[40] (σ_{Break}) and fracture toughness[35] (G_C). The latter quantity was calculated from the Greensmith formulation[41] for fracture toughness in elastomeric notched samples, with w_0 being fracture energy for the unnotched sample up to the strain at break of the notched one, W_C the notch width and λ the stretch ratio at break of the notched specimen:

$$G_C = \frac{6 w_0 W_C}{\sqrt{\lambda}} \quad (2)$$

Self-healing efficiency (η) was calculated as the ratio of the considered mechanical property between the healed and virgin states:

$$\eta_\sigma = \frac{\sigma_{Break,Healed}}{\sigma_{Break,Virgin}} \times 100 \quad (3)$$

$$\eta_{G_C} = \frac{G_{C\,Healed}}{G_{C\,Virgin}} \times 100 \quad (4)$$

Under the room temperature/low humidity set of conditions, the material was evaluated after 3, 7, and 14 days of exposure. Recovery of the original stress–strain curve (Figure 6) was limited, as the set temperature (21°C) was lower than blend glass transition, resulting in hindered macromolecular mobility by the presence of the frozen hard phase.

Healing efficiency increased together with healing time, as seen in Figure 7. For tensile strength, a 26% recovery was recorded after 3 days, rising to 39% and 47% after 7 and 14 days, respectively. Fracture toughness recovery achieved lower values overall. This result can find an explanation by considering this data as more dependent on chain interdiffusion across the damaged interface, with the consequence of being more susceptible to motion restriction by the hard phase.

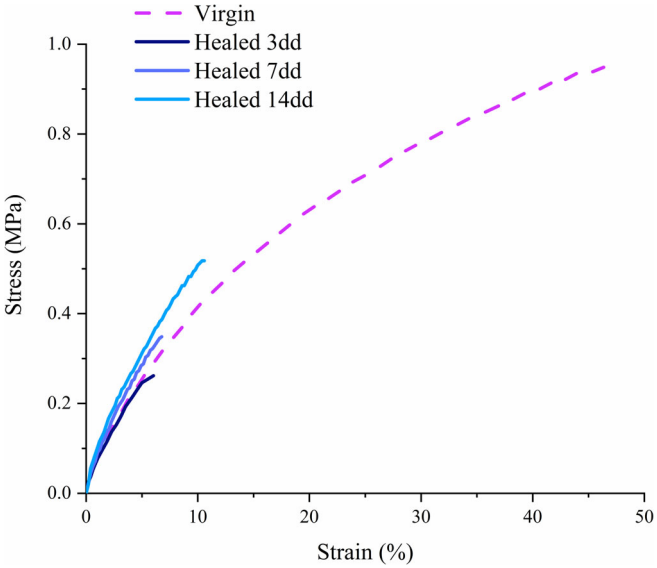

FIGURE 6 Stress–strain curves for PUU CAT1.5-ANC1.5 at virgin and after 3-, 7-, and 14-days healing (21°C, 30% RH)

Literature suggests the influence of water, in liquid form or as water vapor, on the self-healing capabilities of ionic supramolecular polymers.[24,31] Its presence at the damage interface is supposed to generate dipole–dipole interactions with polymer ionic clusters, which would then migrate toward the exposed surface. The proximity between oppositely charged functionalities increases the intensity of supramolecular interactions, accelerating chain diffusion across the interface and material integrity restoration.

Data for healing efficiency versus healing time from Figure 8 show a significant improvement in tensile strength recovery, achieving a 66% efficiency at 7 days. Fracture toughness increased even above its starting value as a consequence of the plasticizing effect of the water absorbed from the high humidity environment.

As the T_g for the system presented here is around 35°C, healing in an oven at 50°C proved to be a fast and effective method to achieve sufficient recovery of mechanical properties (Figure 9). Tensile strength showed complete recovery after only 1 h, the same result as for fracture toughness. The latter also presented a significant increase above its original value as the heating cycle affected the material microstructural organization, extending the elastomer plastic region and increasing its fracture energy.

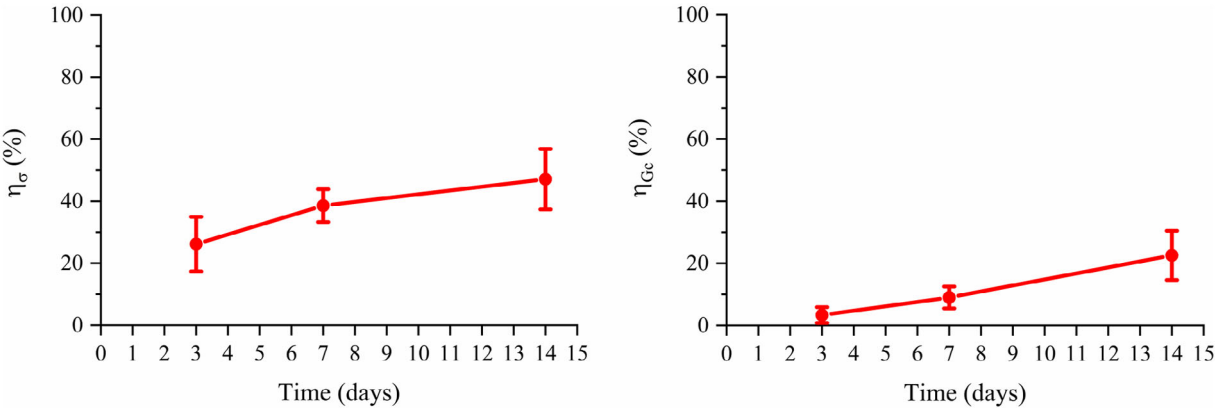

FIGURE 7 Healing efficiency for PUU CAT1.5-ANC1.5 at different healing times at 21°C and 30% RH for tensile strength (left) and fracture toughness (right)

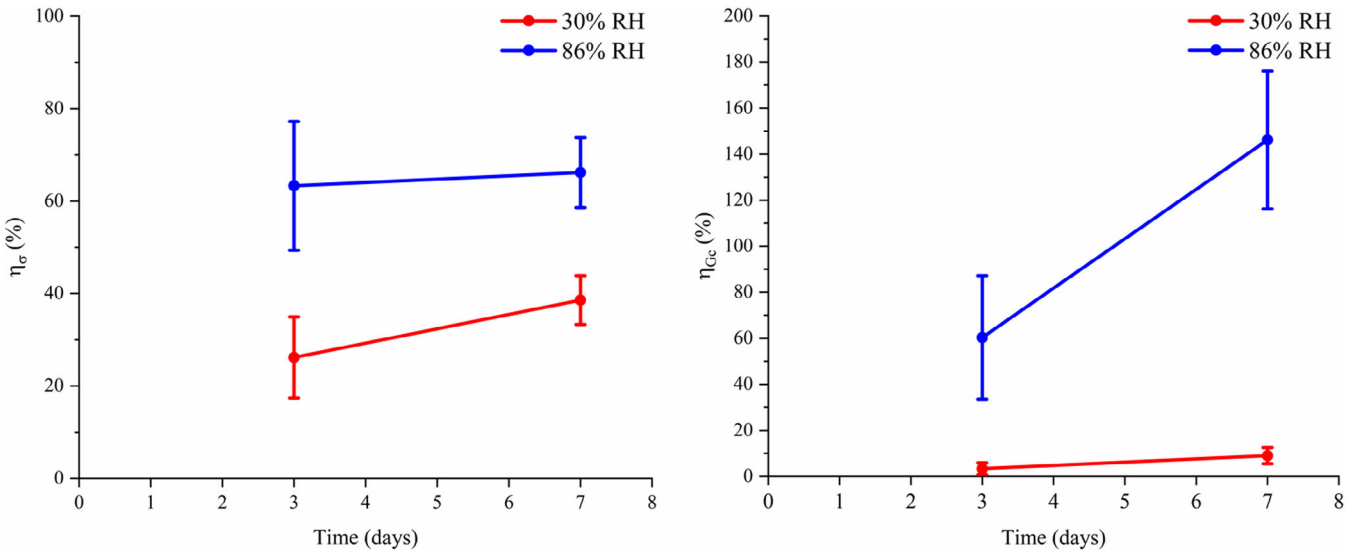

FIGURE 8 Healing efficiency for PUU CAT1.5-ANC1.5 at different healing times at 21°C and 30% RH (red) and 86% RH (blue) for tensile strength (left) and fracture toughness (right)

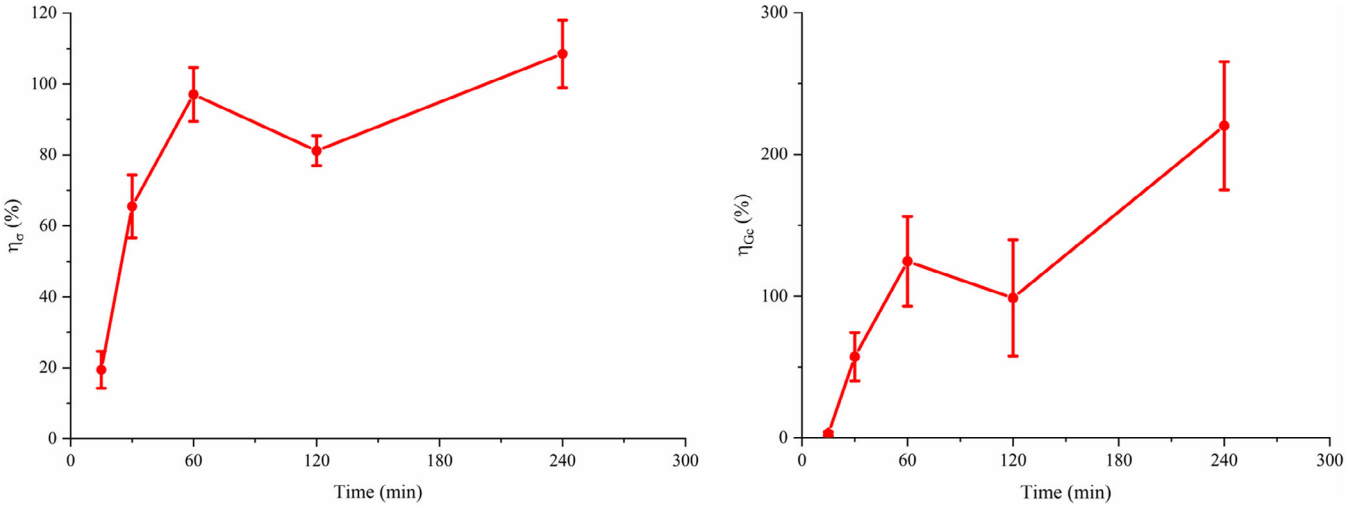

FIGURE 9 Healing efficiency for PUU CAT1.5-ANC1.5 at different healing times at 50°C for tensile strength (left) and fracture toughness (right)

4 | CONCLUSIONS

The synthesis of raw ionomers consisted of a two-step reaction between PDMS amine-terminated, IPDI, and different chain extenders, depending on the ionic functionality desired. The significant difference between the solubility parameters of PDMS and urea/urethane functionalities induced at a partial phase separation, resulting in a segmented nature and elastomeric behavior.

The blending of the synthesized anionomer and cationomer resulted in a material retaining the original elastomeric behavior, coupled with enhanced supramolecular cohesion. This microstructure and supramolecular interactions led to a higher T_g, increasing from 23°C measured for the cationomer to nearly 35°C for the poly(urea-urethane) blend.

The formation of ionic interactions was evidenced by the differences between FT-IR spectra, mechanical and rheological properties of pure and blended ionomers. Stress–strain curves presented a more fragile behavior for the blend and a significant increase in tensile strength from 0.34 MPa for the cationomer to 1.11 MPa for the poly(urea-urethane) blend. The rheological analysis showed the limitations imposed on electrostatic attraction by phase separation. Below T_g, the blend behaved as a homogeneous polymer mixture, with a value of G' intermediate between that of the pure ionomers. Nevertheless, above T_g, the value of G' recorded for the blend was 0.29 MPa, against 0.13 MPa and 0.08 MPa for the anionomer and the cationomer, respectively. This demonstrates that, with sufficient conformational freedom and molecular mobility, oppositely charged functionalities were able to aggregate more extensively into ionic clusters, improving the supramolecular cohesion by noncovalent crosslinking.

The dynamic and reversible nature of the described supramolecular interactions triggered self-recovery in damaged samples. The material showed hints of self-restoration capabilities at room temperature, without external contribution, achieving 47% recovery of tensile strength at 14 days. Additionally, further studies performed with different environmental conditions allowed a better understanding of their influence on the healing phenomenon. Both humidity and heating allowed to overcome the limitations imposed by restricted molecular mobility on the recovery of pristine properties. The humidity in particular promoted ionic moieties migration toward the exposed surface, increasing the strength of their reciprocal electrostatic attraction. High relative humidity in the atmosphere (86% RH) caused the tensile strength self-healing efficiency to almost double up from 37% to 66% at 7 days, while moderated heating at 50°C resulted in the achievement of complete recovery of the original properties after 1 h of treatment only. An identical trend was observed in the fracture toughness recovery. As fracture toughness is a descriptor of cohesive forces acting in the polymer bulk more complete than the tensile strength, these trends can be taken as additional proof of restored supramolecular interactions after the material failure.

These remarkable results therefore can be taken as a reference in pursuing the development of new ionic polyurethane blends with self-healing abilities and able to form interpenetrating polymer networks (IPN) based on supramolecular ionic interactions.

ACKNOWLEDGMENT

Open Access Funding provided by Politecnico di Milano within the CRUI-CARE Agreement.

DATA AVAILABILITY STATEMENT

The data that support the findings of this study are available from the corresponding author upon reasonable request.

ORCID

Federico Da Via https://orcid.org/0000-0002-8473-0347
Raffaella Suriano https://orcid.org/0000-0002-7448-359X
Oussama Boumezgane https://orcid.org/0000-0003-2602-6279
Antonio M. Grande https://orcid.org/0000-0003-4913-2525

REFERENCES

1. Destrade C, Mondon-Bernaud MC, Tinh NH. Mesomorphic polymorphism in some disc-like compounds. *Mol Cryst Liq Cryst*. 1979;49(6):169-174. https://doi.org/10.1080/00268947908070455
2. Fouquey C, Lehn J-M, Levelut A. Molecular recognition directed self-assembly of supramolecular liquid crystalline polymers from complementary chiral components. *Adv Mater*. 1990;2(5):254-257. https://doi.org/10.1002/adma.19900020506
3. Dobrawa R, Würthner F. Metallosupramolecular approach toward functional coordination polymers. *J Polym Sci Part A Polym Chem*. 2005;43(21):4981-4995. https://doi.org/10.1002/pola.20997
4. Hosseini MW, Ruppert R, Schaeffer P, De Cian A, Kyritsakas N, Fischer J. A molecular approach to solid-state synthesis: prediction and synthesis of self-assembled infinite rods. *J Chem Soc Chem Commun*. 1994;18:2135-2136. https://doi.org/10.1039/c39940002135
5. Felix O, Hosseini MW, De Cian A. Design of 2-D hydrogen bonded molecular networks using pyromellitate dianion and cyclic bisamidinium dication as complementary tectons. *Solid State Sci*. 2001;3(7):789-793. https://doi.org/10.1016/S1293-2558(01)01202-X
6. Bazuin CG, Eisenberg A. Modification of polymer properties through ion incorporation. *Ind Eng Chem Prod Res Dev*. 1981;20(2):271-286. https://doi.org/10.1021/i300002a010
7. Eisenberg A, Hird B, Moore RB. A new multiplet-cluster model for the morphology of random ionomers. *Macromolecules*. 1990;23(18):4098-4107. https://doi.org/10.1021/ma00220a012
8. Król P. Synthesis methods, chemical structures and phase structures of linear polyurethanes. Properties and applications of linear polyurethanes in polyurethane elastomers, copolymers and ionomers. *Prog Mater Sci*. 2007;52(6):915-1015. https://doi.org/10.1016/j.pmatsci.2006.11.001
9. Charnetskaya AG, Polizos G, Shtompel VI, Privalko EG, Kercha YY, Pissis P. Phase morphology and molecular dynamics of a polyurethane ionomer reinforced with a liquid crystalline filler. *Eur Polym J*. 2003;39(11):2167-2174. https://doi.org/10.1016/S0014-3057(03)00136-8
10. Zhu Y, Hu J, Lu J, Yeung LY, Yeung K. Shape memory fiber spun with segmented polyurethane ionomer. *Polym Adv Technol*. 2008;19(12):1745-1753. https://doi.org/10.1002/pat
11. Fragiadakis D, Dou S, Colby RH, Runt J. Molecular mobility, ion mobility and mobile ion concentration in poly(ethylene oxide)-based polyurethane ionomers. *Macromolecules*. 2008;41(15):5723-5728. https://doi.org/10.1021/ma800263b
12. Kakati DK, George MH. Polyurethane ionomers containing phosphate groups. *Polymer (Guildf)*. 1993;34(20):4319-4324. https://doi.org/10.1016/0032-3861(93)90195-G
13. Jaisankar SN, Anandprabu A, Lakshminarayana Y, Radhakrishnan G. Preparation and properties of semi-interpenetrating polymer networks based on polyurethane ionomer/polyvinyl chloride. *J Mater Sci*. 2000;35(5):1065-1068. https://doi.org/10.1023/A:1004778707828

14. Cakic SM, Stamenkovic JV, Djordjevic DM, Ristic IS. Synthesis and degradation profile of cast films of PPG-DMPA-IPDI aqueous polyurethane dispersions based on selective catalysts. *Polym Degrad Stab*. 2009;94(11):2015-2022. https://doi.org/10.1016/j.polymdegradstab.2009.07.015
15. Wang L, Yang B, Wang XL, Tang XZ. A novel polymer electrolyte based on polydioxolane polyurethane with Na+ single-ionic conductivity. *J Appl Polym Sci*. 1999;71(10):1711-1719. https://doi.org/10.1002/(SICI)1097-4628(19990307)71:10⟨1711::AID-APP18⟩3.0.CO;2-Y
16. Zhu W, Wang XL, Yang B, Wang L, Tang XZ, Yang C. Synthesis and characterization of polydioxolane polyurethane ionomer. *J Mater Sci*. 2001;36(21):5137-5141. https://doi.org/10.1023/A:1012481409241
17. Robila G, Buruiana T, Buruiana EC. Synthesis and properties of some polyurethane anionomers with carboxylate groups. *Eur Polym J*. 1999;35(7):1305-1311. https://doi.org/10.1016/s0014-3057(98)00208-0
18. Hwang KKS, Yang C, Cooper SL. Properties of polyether-polyurethane zwitterionomers. *Polym Eng Sci*. 1981;21(15):1027-1036. https://doi.org/10.1002/pen.760211509
19. Yang C, Hwang KKS, Cooper SL. Morphology and properties of polybutadiene- and polyether-polyurethane zwitterionomers. *Die Makromol Chemie*. 1983;184(3):651-668. https://doi.org/10.1002/macp.1983.021840318
20. Speckhard TA, Hwang KKS, Yang C, Laupan WR, Cooper SL. Properties of segmented polyurethane zwitterionomer elastomers. *J Macromol Sci Part B*. 1984;23(2):175-199. https://doi.org/10.1080/00222348408219455
21. Yu X-H, Nagarajan MR, Grasel TG, Gibson PE, Cooper SL. Polydimethylsiloxane-polyurethane elastomers: synthesis and properties of segmented copolymers and related zwitterionomers. *J Polym Sci Polym Phys Ed*. 1985;23(11):2319-2338. https://doi.org/10.1002/pol.1985.180231106
22. Yang C, Li C, Cooper SL. Synthesis and characterization of polydimethylsiloxane polyurea-urethanes and related zwitterionomers. *J Polym Sci Part B Polym Phys*. 1991;29(1):75-86. https://doi.org/10.1002/polb.1991.090290110
23. Chen S, Mo F, Yang Y, et al. Development of zwitterionic polyurethanes with multi-shape memory effects and self-healing properties. *J Mater Chem A*. 2015;3(6):2924-2933. https://doi.org/10.1039/c4ta06304j
24. Wen H, Chen S, Ge Z, Zhuo H, Ling J, Liu Q. Development of humidity-responsive self-healing zwitterionic polyurethanes for renewable shape memory applications. *RSC Adv*. 2017;7(50):31525-31534. https://doi.org/10.1039/c7ra05212j
25. Comí M, Lligadas G, Ronda JC, Galià M, Cádiz V. Adaptive bio-based polyurethane elastomers engineered by ionic hydrogen bonding interactions. *Eur Polym J*. 2017;91(April):408-419. https://doi.org/10.1016/j.eurpolymj.2017.04.026
26. Dodge L, Chen Y, Brook MA. Silicone boronates reversibly crosslink using Lewis Acid-Lewis Base amine complexes. *Chem—A Eur J*. 2014;20(30):9349-9356. https://doi.org/10.1002/chem.201402877
27. Zepeda-Velazquez L, Macphail B, Brook MA. Spread and set silicone-boronic acid elastomers. *Polym Chem*. 2016;7(27):4458-4466. https://doi.org/10.1039/c6py00492j
28. Mahesh GN, Ramesh S, Radhakrishnan G. Study of ionomer blends based on a polyurethane cationomer and an acrylic anionomer. *Macromol Rapid Commun*. 1996;17(2):73-80. https://doi.org/10.1002/marc.1996.030170201
29. Liu Z, Hong P, Huang Z, et al. Self-healing, reprocessing and 3D printing of transparent and hydrolysis-resistant silicone elastomers. *Chem Eng J*. 2020;387(January):124142. https://doi.org/10.1016/j.cej.2020.124142
30. Xiao Y, Huang H, Peng X. Synthesis of self-healing waterborne polyurethanes containing sulphonate groups. *RSC Adv*. 2017;7(33):20093-20100. https://doi.org/10.1039/C6RA28416G
31. Hu X, Xu S, Feng S, Wang J, Xu J. Saline-enabled self-healing of polyelectrolyte multilayer films. *RSC Adv*. 2015;5(12):8877-8881. https://doi.org/10.1039/c4ra13373k
32. Han Q, Urban MW. Kinetics and mechanisms of catalyzed and non-catalyzed reactions of OH and NCO in acrylic polyol-1,-6-hexamethylene diisocyanate (HDI) polyurethanes. VI. *J Appl Polym Sci*. 2002;86(9):2322-2329. https://doi.org/10.1002/app.11251
33. Sheth JP, Aneja A, Wilkes GL, et al. Influence of system variables on the morphological and dynamic mechanical behavior of polydimethylsiloxane based segmented polyurethane and polyurea copolymers: a comparative perspective. *Polymer (Guildf)*. 2004;45(20):6919-6932. https://doi.org/10.1016/j.polymer.2004.06.057
34. Suriano R, Boumezgane O, Tonelli C, Turri S. Viscoelastic properties and self-healing behavior in a family of supramolecular ionic blends from silicone functional oligomers. *Polym Adv Technol*. 2020;31(12):3247-3257. https://doi.org/10.1002/pat.5049
35. Bode S, Enke M, Hernandez M, et al. Characterization of self-healing polymers: from macroscopic healing tests to the molecular mechanism. *Advances in Polymer Science*. Vol 5. Springer; 2015:113-142. https://doi.org/10.1007/12_2015_341
36. Keller MW, White SR, Sottos NR. A self-healing poly(dimethyl siloxane) elastomer. *Adv Funct Mater*. 2007;17(14):2399-2404. https://doi.org/10.1002/adfm.200700086
37. Maes F, Montarnal D, Cantournet S, Tournilhac F, Corté L, Leibler L. Activation and deactivation of self-healing in supramolecular rubbers. *Soft Matter*. 2012;8(5):1681-1687. https://doi.org/10.1039/c2sm06715c
38. Grande AM, Garcia SJ, van der Zwaag S. On the interfacial healing of a supramolecular elastomer. *Polymer (Guildf)*. 2015;56:435-442. https://doi.org/10.1016/j.polymer.2014.11.052
39. Grande AM, Bijleveld JC, Garcia SJ, van der Zwaag S. A combined fracture mechanical – rheological study to separate the contributions of hydrogen bonds and disulphide linkages to the healing of poly(urea-urethane) networks. *Polymer (Guildf)*. 2016;96:26-34. https://doi.org/10.1016/j.polymer.2016.05.004
40. Bekas DG, Tsirka K, Baltzis D, Paipetis AS. Self-healing materials: a review of advances in materials, evaluation, characterization and monitoring techniques. *Compos Part B Eng*. 2016;87:92-119. https://doi.org/10.1016/j.compositesb.2015.09.057
41. Greensmith HW. Rupture of rubber. X. The change in stored energy on making a small cut in a test piece held in simple extension. *J Appl Polym Sci*. 1963;7(3):993-1002. https://doi.org/10.1002/app.1963.070070316

How to cite this article: Da Via F, Suriano R, Boumezgane O, Grande AM, Tonelli C, Turri S. Self-healing behavior in blends of PDMS-based polyurethane ionomers. *Polym Adv Technol*. 2022;33(2):556-565. doi:10.1002/pat.5537